Experimental report

16/10/2020

Proposal: 5-14-268 **Council:** 4/2019

Title: Neutron diffraction study on the lattice of thermoelectric material Ag8SnSe6

Research area: Materials

This proposal is a continuation of 5-14-263

Main proposer: Qingyong REN

Experimental team: Dimitri RENZY
Qingyong REN
Jiangtao WU

Local contacts: Oscar Ramon FABELO ROSA
Jose Alberto RODRIGUEZ VELAMAZAN

Samples: Ag8SnSe6

Instrument	Requested days	Allocated days	From	To
D9	6	6	16/09/2019	23/09/2019

Abstract:

Ag8SnSe6 compounds are a group of promising thermoelectric materials. One main feature of this material as thermoelectric candidate is the ultra-low thermal conductivity. One possible reason is the weak bonding of Ag ions and complex unit cell. Another explanation is the liquid phonon behavior above the phase transition around 350 K. In our previous experiment, we have studied the cubic structure above the phase transition temperature, and found a quasi-liquid phonon behavior. In this proposal, we would like to study the structure below and around the phase transition temperature. This results would be helpful to understand the relationship between the thermal conductivity, structures and phase transitions in the Ag8SnSe6.

Ultralow lattice thermal conductivity in Ag_8SnSe_6 thermoelectric material

Qingyong Ren (2019.11.19)

1. Background

The demand for sustainable energies has motivated a great many of researches on different types of energy conversion technologies in the past decades. Thermoelectrics, which can directly convert heat into electricity, is considered to have potential application in energy harvesting. The efficiency of this energy conversion process is quantified by the thermoelectric figure of merit, $zT = \sigma S^2 T/(\kappa_{ele} + \kappa_{lat})$, where σ, S, T, κ_{ele}, and κ_{lat} are the electric conductivity, the Seebeck coefficient, the absolute temperature, and the electronic and lattice contributions to the thermal conductivity, respectively [1]. It is straightforward from this formula that the thermoelectric performance could be optimized by tailoring the electronic properties (electronic conductivity and Seebeck coefficient), and by suppressing the thermal conductivity, κ (=κ_{ele} + κ_{lat}), as much as possible. σ, S, and κ_{ele} strongly couple with each other, and this make it difficult to improve zT through tune these three parameters. Alternatively, suppressing κ_{lat} is an important and effective strategy [2, 3]. The lattice thermal conductivity can be described by $\kappa_{\mathrm{lat}} = 1/3cv^2\tau = 1/3cvl$,where c, v, τ and l are heat capacity, phonon velocity, phonon mean free path and phonon relaxation time, respectively [4]. κ_{lat} can be lowered by suppressing any of these three parameters.

Recently, the argyrodite-type $A_{(12-n)/m}{}^{m+}B^{n+}X_6{}^{2-}$ compounds (A^{m+} = Li^+, Cu^+, or Ag^+, B^{n+} = Ga^{3+}, Si^{4+}, Ge^{4+}, Sn^{4+}, P^{5+}, or As^{5+}, and X = S, Se, or Te) have received a great many of attentions as a group of promising thermoelectric materials with ultralow lattice thermal conductivities [5-11]. One possible reason for the ultralow lattice thermal conductivity in argyrodite-type materials is the large unit cell with complex structure and weak chemical bonds [10, 11]. One alternative explanation is that the argyrodite-type samples exhibits liquid-like superionic behavior [8, 9]. As a typical example, Ag_8SnSe_6 exhibit a phase transition from the low-temperature β-Ag_8SnSe_6 (space group $Pmn2_1$) to the high-temperature γ-Ag_8SnSe_6 (space group $F\text{-}43m$) [12, 13]. Above the transition temperature, the Ag^+ cations distribute at three different atomic positions. The non-fully-occupied states of Ag^+ allow it jump between different sites. This diffusive behavior of Ag^+ in the $SnSe_6$-sublattice would damp the transverse phonon vibration. To unveil the underlying mechanisms that engender an ultralow lattice thermal conductivity in Ag_8SnSe_6, we designed to take neutron single crystal diffraction measurements.

2. Experimental details

Ag_8SnSe_6 single crystal was grown by Bridgeman methods. The crystal structure was checked using x-ray powder diffraction. In addition, Laue backscattering measurement was used to align the single crystal. Single crystal neutron diffraction experiments were carried out using the Hot Neutron 4-circle Diffractometer (D9) at the Institut Laue-Langevin. The sample was measured at four different temperature points, 90 K and 300 K (this experiment) and 400 K and 650 K (the previous experiment). The data was analyzed using Rietveld refinement method [14, 15] and maximum entropy method (MEM) [16, 17].

3. Results and analysis

Fig. 1 shows the crystal structure and the neutron scattering-length densities determined by Rietveld and MEM analysis of neutron diffraction data at 300 K. The sample crystallize into a orthorhombic structure with $Pmn2_1$. According to the MEM analysis as shown in Fig. 1(b), Ag^+ ions in the orthorhombic structure exhibit well defined atomic positions.

Fig. 2 shows the crystal structure and the neutron scattering-length densities determined by Rietveld and MEM analysis of neutron diffraction data at 400 K. The sample crystallize into a cubic structure

with *F-43m*. The neutron scattering-length densities projected along the <111> directions are shown in Fig. 2(b). This contour image demonstrated a localized diffusion of Ag^+ cations between the two 48*h* positions.

For more information about the structures below and above the transition temperature, please see the Tables 1.

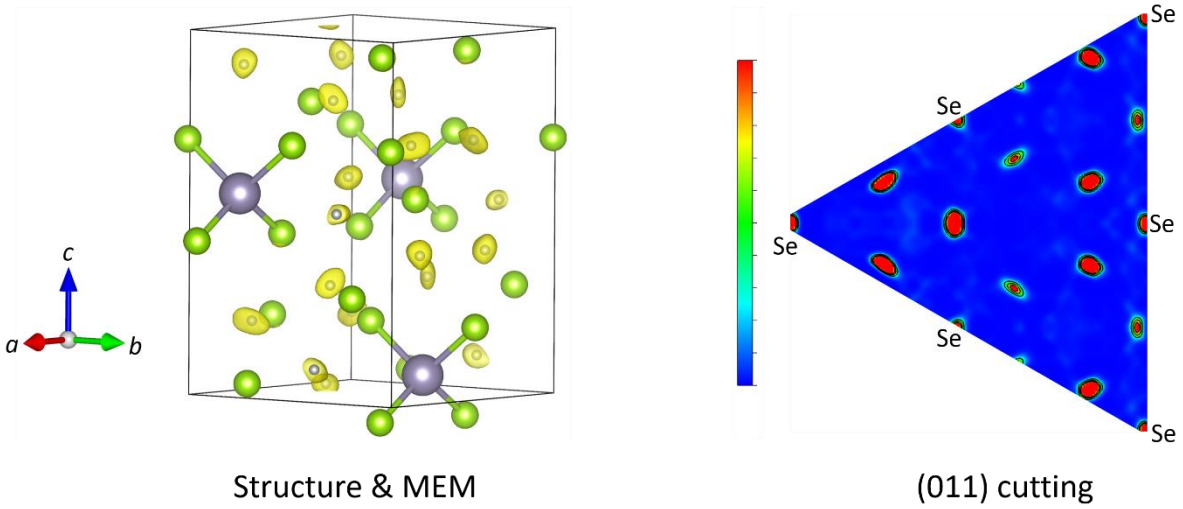

Fig. 1 Isosurfaces of the neutron scattering-length densities determined by maximum entropy analysis of neutron diffraction data and corresponding projection along [011] at 300 K. Except the contribution from the Se (4*a*) atoms, all the other density shown in (b) comes from the Ag atoms.

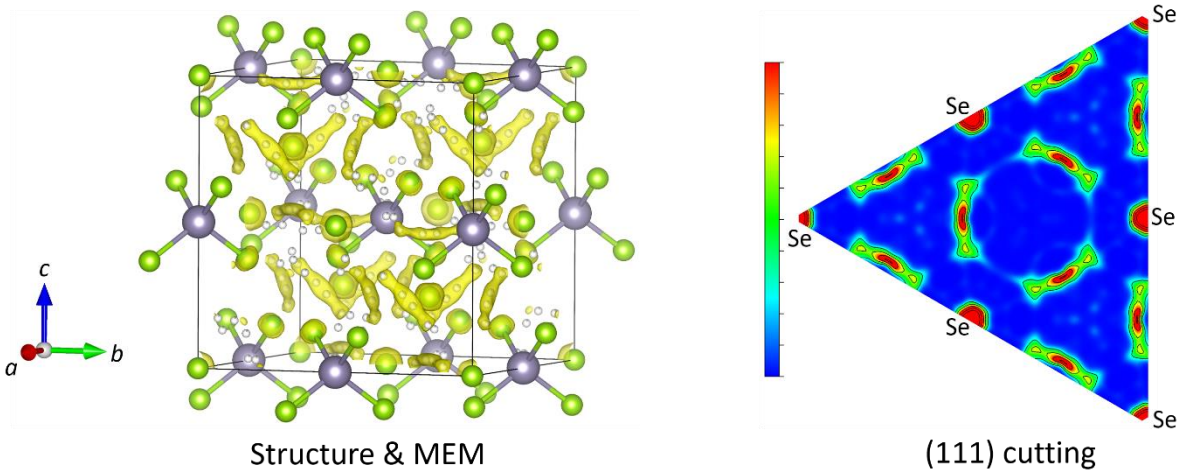

Fig. 2 Isosurfaces of the neutron scattering-length densities determined by maximum entropy analysis of neutron diffraction data and corresponding projection along [111] at 400 K. Except the contribution from the Se (4*a*) atoms, all the other density shown in (b) comes from the Ag atoms.

Table 1. Crystallographic data for Ag_8SnSe_6

Temperature (K)	90	300	400	650
Space group	$Pmn2_1$	$Pmn2_1$	*F-43m*	*F-43m*
Unit cell *a* (Å)	7.9066	7.9088	11.1384	11.2019
b (Å)	7.7792	7.8210		
c (Å)	10.9825	11.0516		
V (Å^3)	675.5049	683.5926	1381.8740	1405.6431
Z	2	2	4	4
ρ_{calc} (g cm^{-3})	7.156	7.071	7.001	6.884
λ (Å)	0.837	0.837	0.837	0.837
θ_{max} (deg)	77.83	77.83	150	150
Reflection collected	1323	1507	563	388
R_{int} (%)	0.39	1.28	7.6	2.5
Unique reflections	1307	1307	357	353
Parameters refined	80	80	31	31
R (%)	6.54	7.59	5.80	10.5
R_w (%)	5.79	5.15	3.15	8.37
Goodness of fit	12.2	6.07	1.94	1.45

References

[1] G. J. Snyder and E. S. Toberer, *Nat. Mater.* **7**, 105 (2008).
[2] O. Delaire, J. Ma, K. Marty, A. F. May, M. A. McGuire, M. H. Du, D. J. Singh, A. Podlesnyak, G. Ehlers, M. D. Lumsden and B. C. Sales, *Nat. Mater.* **10**, 614 (2011).
[3] J. Ma, O. Delaire, A. F. May, C. E. Carlton, M. A. McGuire, L. H. VanBebber, D. L. Abernathy, G. Ehlers, T. Hong, A. Huq, W. Tian, V. M. Keppens, Y. Shao-Horn and B. C. Sales, *Nat. Nanotechnol.* **8**, 445 (2013).
[4] E. S. Toberer, A. Zevalkink and G. J. Snyder, *J. Mater. Chem.* **21**, 15843 (2011).
[5] W. F. Kuhs, R. Nitsche and K. Scheunemann, *Mater. Res. Bull.* **14**, 241 (1979).
[6] L. Li, Y. Liu, J. Dai, A. Hong, M. Zeng, Z. Yan, J. Xu, D. Zhang, D. Shan, S. Liu, Z. Ren and J.-M. Liu, *J. Mater. Chem. C* **4**, 5806 (2016).
[7] W. Li, S. Lin, B. Ge, J. Yang, W. Zhang and Y. Pei, *Adv Sci (Weinh)* **3**, 1600196 (2016).
[8] B. Jiang, P. Qiu, H. Chen, Q. Zhang, K. Zhao, D. Ren, X. Shi and L. Chen, *Chem. Commun.* **53**, 11658 (2017).
[9] B. Jiang, P. Qiu, E. Eikeland, H. Chen, Q. Song, D. Ren, T. Zhang, J. Yang, B. B. Iversen, X. Shi and L. Chen, *J. Mater. Chem. C* **5**, 943 (2017).
[10] S. Lin, W. Li, S. Li, X. Zhang, Z. Chen, Y. Xu, Y. Chen and Y. Pei, *Joule* **1**, 816 (2017).
[11] W. Li, S. Lin, M. Weiss, Z. Chen, J. Li, Y. Xu, W. G. Zeier and Y. Pei, *Adv. Energy Mater.*, 1800030 (2018).
[12] J. P. Deloume, R. Faure, H. Loiseleur and M. Roubin, *Acta Crystallographica Section B* **34**, 3189 (1978).
[13] J.-P. Deloume and R. Faure, *J. Solid State Chem.* **36**, 112 (1981).
[14] H. Rietveld, *J. Appl. Crystallogr.* **2**, 65 (1969).
[15] J. Rodríguez-Carvajal, *Commission on powder diffraction (IUCr). Newsletter* **26**, 12 (2001).
[16] S. M. and S. M., *Acta Crystallographica Section A* **46**, 263 (1990).
[17] K. Momma, T. Ikeda, A. A. Belik and F. Izumi, *Powder Diffr.* **28**, 184 (2013).